Hindawi
Mathematical Problems in Engineering
Volume 2020, Article ID 3194196, 11 pages
https://doi.org/10.1155/2020/3194196

Research Article

Sizing Optimization and Experimental Verification of a Hybrid Generation Water Pumping System in a Greenhouse

Dan Li,[1,2] Delan Zhu ,[1,2] Ruixin Wang,[3] Maosheng Ge,[1,2] Shoujun Wu,[1,2] and Yaohui Cai[1,2]

[1]*Key Laboratory of Agricultural Soil and Water Engineering in Arid and Semiarid Areas, Ministry of Education, Northwest A&F University, Yangling 712100, Shaanxi, China*
[2]*College of Water Resources and Architectural Engineering, Northwest A&F University, Yangling 712100, Shaanxi, China*
[3]*Industrial Engineering, Purdue University, West Lafayette 47906, IN, USA*

Correspondence should be addressed to Delan Zhu; xnylsx@nwafu.edu.cn

Received 27 December 2019; Revised 7 April 2020; Accepted 21 April 2020; Published 11 May 2020

Academic Editor: Fausto Arpino

Copyright © 2020 Dan Li et al. This is an open access article distributed under the Creative Commons Attribution License, which permits unrestricted use, distribution, and reproduction in any medium, provided the original work is properly cited.

In remote agricultural areas, electrical energy is usually deficient for pumping water into greenhouses. Photovoltaic (PV) panels and wind generators are considered suitable options for power supply. The reliability of hybrid generation water pumping depends primarily on the number of system components, which should be adapted to the local climatic conditions and crop irrigation schedule. In this study, a universal size optimization model is established to optimize the configuration of a hybrid PV-wind-battery (PWB) generation system. The climatic conditions and crop irrigation schedule are parameterized in the model. Minimization of the annual cost of the hybrid PWB system is the objective function. The constraints include the battery state of charge (S_{OC}) and the power supply reliability, which consists of the loss of power supply (δ_{LPS}) and the excess energy (δ_{EX}). The numbers of PV panels and batteries, as well as the rated power of the wind generator, are the decision variables. The optimization model of the PWB generation system is solved using a particle swarm optimization (PSO) algorithm based on penalty function. The model is then applied to determine the optimal configuration of a water pumping system for a greenhouse used to grow tomatoes. Measured climatic data are used in the optimization process, which is conducted in the month of maximum irrigation water requirement (August). The optimal results for this greenhouse are two PV panels and two batteries, and the rated power of the wind generator is 375 W. Furthermore, field experiments are performed to validate the optimization model. The field experiment results show that the total output power of the PV panels and wind generator during 15 d are 41.478 kW and 6.235 kW, respectively. The total load power of the pump is 36.965 kW. The field experiments demonstrate that the optimal results are able to meet the power requirements of the water pumping system and the sizing optimization model is appropriate.

1. Introduction

In remote agricultural areas, limited electricity is one of the most crucial issues and it is common to use diesel generators to supply electricity for water pumping systems [1, 2]. However, due to the instability of fuel prices, the use of renewable energy has become an important option that could solve the energy shortage crisis and ensure sustainable development [3]. Photovoltaic (PV) and wind energy are often abundant in remote areas [4, 5] and have been widely used in agricultural applications [6–8]. In addition, renewable energy sources have many advantages, namely, low generation costs, availability, and environmental friendly [9–11]. However, there are issues associated with the instability and intermittent nature of solar and wind energy, and the high initial investment, as well as the low conversion efficiency of PV panels and wind generators [12–14]. It is difficult to ensure reliable electricity supply and minimize the cost of the hybrid PV-wind-battery (PWB) generation system. The devices in the system have to be sized appropriately [15, 16]. Therefore, the optimization of hybrid PWB generation system is crucial to ensure reliable water pumping performance at low cost.

Various methods have been developed to establish the optimization model of the PWB system [17–19]. For example, Muhsen et al. [19] proposed sizing algorithms based

on the minimization of cost functions using the loss of load probability concept. Shrestha and Goel [20] focused on developing analytical methods based on a simple calculation of the PV modules' surface and the battery's capacity using the energetic balance method. Zhang et al. [21] focused on the cost versus reliability issue by determining the optimal size of the system elements from an economic point of view. Tégani et al. [22] proposed a methodology for an optimal sizing design and strategy control based on a differential flatness approach, which was applied to a hybrid stand-alone PV-wind system. A multiobjective techno-economic optimization approach based on the LINGO software was used to ensure the optimum configuration between two conflicting objectives such as the system reliability and cost optimizations [23].

Moreover, many conventional optimization methods have been used for hybrid PWB systems. The linear programming model, mixed-integer linear programming, and iterative techniques are examples of classical algorithms that have been widely used for optimizing hybrid PWB systems [24]. In addition, Maleki [25] employed the improved bee algorithm and harmony search algorithm to optimize the design of six grid-independent hybrid renewable energy systems. The results demonstrated that the improved bee algorithm showed significant promise. Zhang et al. [26] presented an efficient method based on a heuristic procedure for the optimization of an independent off-grid hybrid system. The simulation results showed that the heuristic procedure was more promising than the harmony search and annealing methods. A new hybrid optimization algorithm based on three algorithms was proposed for the optimal configuration of a stand-alone off-grid hybrid PV and wind energy system. The simulation results demonstrated the advantages of the hybrid optimization algorithm for a stand-alone hybrid renewable energy system [27]. Maleki [28] applied an optimization approach based on evolutionary programming to evaluate the operational and performance cost of a grid-connected hybrid system. An off-grid PV/wind turbine (WT)/fuel cell (FC)/diesel hybrid system with different fuel prices was used to provide electricity in a remote area, and the model was optimized using a discrete simulated annealing algorithm. The simulation results indicated that the PV/diesel/FC hybrid system was the most cost-effective system for power generation [29]. According to the literature, previous studies have made excellent progress in size optimization of the hybrid system. However, some systems may result in an oversized system for one location and an undersized one for another one [30]. The oversized system not only increases the reliability but also increases financial cost, while the undersized sacrifices reliability for system economics. Thus, the system size must be carefully selected for each specific application and location. Previous studies have mainly concentrated on the off-grid and grid-connected hybrid systems. Few studies have focused on sizing optimization of hybrid generation systems for agricultural irrigation, especially for different crop irrigation schedule and climatic conditions. Therefore, it is necessary to establish a universal size optimization model for hybrid generation systems for the agricultural irrigation system. In addition, the traditional model-solving algorithms have drawbacks, such as rigid iterations, low flexibility, and long computation times [31]. The particle swarm optimization (PSO) algorithm has been widely used because of their efficient global search solutions, strong robustness, and anti-interference ability [32–35]. Furthermore, it uses a small number of parameters for adjustment, and similar parameters can be used for different applications, making PSO appealing for the optimization of nonlinear functions [36, 37].

Consequently, this work proposes a universal sizing optimization model of a hybrid PWB system to minimize the annual cost of the system. Excess energy and the loss of power supply are used as constrains, and the numbers of PV panels and batteries, as well as the rated power of the wind generator, are the decision variables. The model is solved by the PSO algorithm based on the penalty function. The solar radiation, ambient temperature, wind speed, irrigation duration, and other variables are parameterized in the model. The optimal configurations of the hybrid PWB generation system can be obtained for specific irrigation systems by considering the local climatic conditions and crop irrigation schedule. Field experiments are conducted to validate the optimization model.

2. Modeling of System Components

Figure 1 shows the structure of the hybrid PWB powered drip irrigation system, which comprises an irrigation system and a power supply system. The irrigation system consists of a water pump, pipe networks, and emitters. The power supply system consists of PV panels, batteries, and a hybrid PV-wind controller. Wind and solar sources provide the electrical energy for the water pump to raise water for crop irrigation.

Figure 2 shows the algorithm block diagram for size optimization of large-scale systems. The input parameters include meteorological parameters, load parameters, and the economic and technical specifications of the system. The optimal combinations of the hybrid power system are obtained with the objectives to ensure system reliability and minimize the cost.

2.1. Water Pump Power Requirement Model. The reference evapotranspiration of the greenhouse crop is calculated using the following equation [38]:

$$\mathrm{ET}_0 = \frac{0.408\Delta\left(R_n - G\right) + \gamma\left(1713\left(e_a - e_d\right)/T_m + 273\right)}{\Delta + 1.64\gamma}, \tag{1}$$

where ET_0 is the reference evapotranspiration (mm h^{-1}), Δ is the saturation slope of the vapor pressure curve at temperature T_m (kPa $^{\circ}C^{-1}$), R_n is the monthly average daily net radiation at the grass surface (MJ m^{-2} h^{-1}), G is the monthly average daily soil heat flux density (MJ m^{-2} day^{-1}), γ is the psychrometric constant (kPa $^{\circ}C^{-1}$), e_a is the saturation vapor pressure (kPa), e_d is the monthly average actual daily vapor

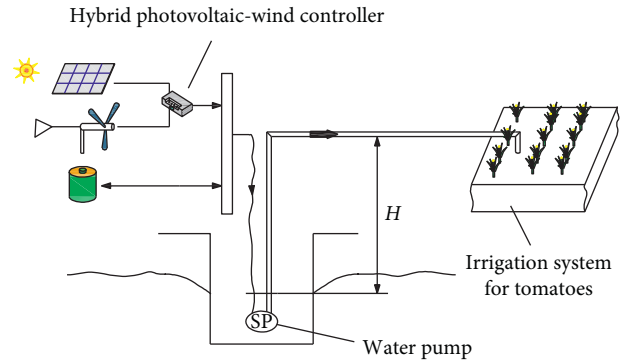

Figure 1: Structure of the hybrid PWB powered drip irrigation system.

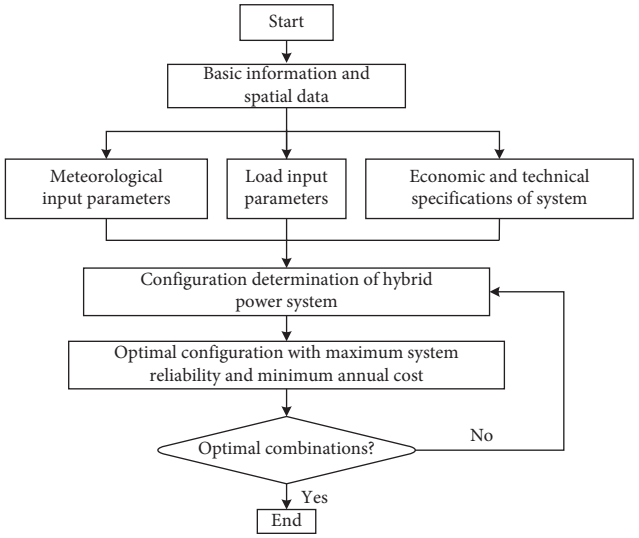

Figure 2: Algorithm block diagram for the size optimization of large-scale systems.

pressure (kPa), and T_m is the monthly average daily air temperature (°C).

The amount of irrigation required by the greenhouse crops is determined by the following equation:

$$I = K_c \mathrm{ET}_0 + \Delta W, \tag{2}$$

where I is the amount of irrigation (mm), K_c is the crop coefficient, and ΔW is the change in soil moisture in the crop root zone (mm).

The flow rate of the water pump is determined by the daily irrigation amount, the irrigation area, and the irrigation duration, as expressed by the following equation:

$$Q = \frac{MA}{1000\, t_c \eta_i}, \tag{3}$$

where Q is the flow rate of the water pump ($m^3\ h^{-1}$), M is the daily irrigation amount (mm), A is the irrigation area (m^2), t_c is the irrigation duration (h), and η_i is the irrigation efficiency (%).

The water pump power is obtained using the following equation:

$$P_{\mathrm{pump}} = \frac{\rho g Q H}{3600 \eta_p}, \tag{4}$$

where P_{pump} is the water pump power (W), ρ is the water density (kg m^{-3}), g is the acceleration of gravity (m s^{-2}), H is the water pump head (m), and η_p is the water pump efficiency (%).

2.2. Wind Generator Output Power Model. For a wind generator, the output power is related to the wind speed. If the wind speed exceeds the cut-out value, the wind generator stops working to protect the generator. The output power of the wind generator is described in terms of the wind speed using the following equation [7, 10, 39]:

$$P_w = \begin{cases} 0, & (v_w \le v_{ci} \text{ or } v_w \ge v_{c0}) \\ P_{w,\mathrm{rate}} \times \dfrac{v_w - v_{ci}}{v_r - v_{ci}}, & (v_{ci} \le v_w < v_r), \\ P_{w,\mathrm{rate}}, & (v_r \le v_w < v_{c0}), \end{cases} \tag{5}$$

where P_w is the output power of the wind generator (W), $P_{w,\mathrm{rate}}$ is the rated power of the wind generator (W), v_w is the current wind speed (m s^{-1}), v_{ci} is the cut-in value for the wind generator (m s^{-1}), v_r is the rated wind speed of the wind generator (m s^{-1}), and v_{co} is the cut-out value for the wind generator (m s^{-1}).

2.3. PV Panel Output Power Model. The power generated by the PV panels is calculated using the following equation:

$$P_{pv} = N_{pv} \eta_{pv} A_{pv} G_{ir}, \tag{6}$$

where P_{pv} is the generated power of the PV panels (W), N_{pv} is the number of PV panels, η_{pv} is the yield from the PV panels (%), A_{pv} is the area of a single PV panel (m^2), and G_{ir} is the solar radiation ($W \cdot m^{-2}$).

The yield model is convenient to use and adaptable to the site characteristics and PV panel technology. In this work, the yield model is chosen to model the PV panels, as defined in the following equation [1, 2, 40]:

$$\eta_{pv} = \eta_r [1 - \beta (T_c - T_{\mathrm{cref}})], \tag{7}$$

where η_r is the PV panel efficiency under the reference conditions (%), β is the temperature coefficient of the PV panel, T_c is the PV panel temperature (°C), and T_{cref} is the reference cell temperature (°C).

The cell temperature T_c, which depends on the ambient temperature T_a and the solar radiation G_{ir}, is calculated using the following equation [1, 2, 40]:

$$T_c = T_a + G_{ir} \left(\frac{\mathrm{NOCT} - 20}{800} \right), \tag{8}$$

where T_a is the ambient temperature (°C) and NOCT is the nominal operation cell temperature (°C).

2.4. Battery Model. Batteries are widely used in hybrid generation systems to store surplus electrical energy and to supply load demand in the case of a deficit of output power from the wind generator and PV panels. Owing to the random nature of power generation by the PV panels and wind generator, the battery capacity constantly changes in hybrid generation systems. Therefore, to describe the charge and discharge process of the battery, the state of charge (S_{OC}) (the ratio between the remaining capacity and the rated capacity of the battery at a certain point in time) is used to describe the remaining capacity of the battery. The battery capacity at time t is calculated by equations (9) and (10):

$$\text{Charge: } S_{OC}(t) = S_{OC}(t - \Delta t) + \frac{\Delta E_{store}\eta_{in}}{N_b E_{rate}}, \quad (9)$$

$$\text{Discharge: } S_{OC}(t) = S_{OC}(t - \Delta t) - \frac{\Delta E_{store}}{\eta_{out} N_b E_{rate}}, \quad (10)$$

where $S_{OC}(t - \Delta t)$ is the capacity of the battery at time $t - \Delta t$ (%), ΔE_{store} is the theoretical charge or discharge capacity of the battery (Wh), η_{in} is the charge efficiency (%), η_{out} is the discharge efficiency (%), N_b is the number of batteries, and E_{rate} is the rated capacity of a single battery (Wh).

The battery capacity of the hybrid generation system should maintain the balance. Thus, when the power generated by the PV panels and the wind generator is lower than the power requirements of the water pump, the battery will discharge to balance the requirements of the pump. The discharge capacity of the battery during the period Δt is calculated by

$$\Delta E_{store} = \frac{\Delta t\left[P_{pump}(t) - P_{pv}(t) - P_w(t)\right]}{\eta_{out}}. \quad (11)$$

Similarly, when the power generated by the PV panels and wind generator is higher than the power requirements of the water pump, the battery will be charged. The charge capacity of the battery during Δt is calculated by using the following equation:

$$\Delta E_{store} = \left[P_{pv}(t) + P_w(t) - P_{pump}(t)\right]\Delta t \eta_{in}. \quad (12)$$

3. Optimization Model

3.1. Objective Function. The objective of the model is to minimize the total annual cost of the hybrid generation system while satisfying the load power requirements and ensuring reliability of the power supply. This objective can be achieved by optimizing the number of PV panels, batteries, and the rated power of the wind generator. The total annual cost includes the initial capital cost, installation cost, and the costs of operation and maintenance [41]. Hence, the objective function is calculated by using the following equation:

$$\text{Minimize: } C_T = C_{acap} + C_{ains} + C_{aom}, \quad (13)$$

where C_T is the total annual cost of the system (RMB), C_{acap} is the annual initial capital cost (RMB), C_{ains} is the annual installation cost (RMB), and C_{aom} is the annual operation and maintenance cost (RMB).

The annual initial capital cost of the system is calculated by using the following equation:

$$C_{acap} = C_{RF}\left(C_{pv}N_{pv} + C_w P_{w,rate} + C_b N_b + C_{con}\right), \quad (14)$$

where C_{RF} is the capital recovery factor, C_{pv} is the unit cost of the PV panel (RMB), C_w is the cost of the wind generator (RMB W^{-1}), C_b is the unit cost of the battery (RMB), and C_{con} is the unit cost of the hybrid PV-wind controller (RMB).

It should be noted that the capital recovery factor is used to convert the total capital cost into the annual capital cost and is calculated by using the following equation [6, 42]:

$$C_{RF} = \frac{d(1+d)^{n_l}}{(1+d)^{n_l} - 1}, \quad (15)$$

where d is the real interest rate (%) and n_l is the project lifetime (years).

In general, the lifetime of a battery is 5 years and the lifetime of a hybrid PV-wind controller is 10 years. Thus, the unit cost of the battery and controller can be calculated using equations (16) and (17):

$$C_b = P_b\left\{1 + S_{FF}\left[\left(\frac{1+f}{1+d}\right)^5 + \left(\frac{1+f}{1+d}\right)^{10} + \left(\frac{1+f}{1+d}\right)^{15}\right]\right\}, \quad (16)$$

$$C_{con} = P_{con}\left[1 + S_{FF}\left(\frac{1+f}{1+d}\right)^{10}\right], \quad (17)$$

where P_b is the battery price (RMB), P_{con} is the controller price (RMB), S_{FF} is the sinking fund factor, and f is the inflation rate (%).

The sinking fund factor is the ratio used to calculate the future value of a series of equal annual cash flows, and it is calculated by using the following equation [10, 43]:

$$S_{FF} = \frac{d}{(1+d)^l - 1}, \quad (18)$$

where l is the lifetime of the battery or solar controller (years).

The annual installation cost, which includes the cost of workmanship, transportation, wiring, and other miscellaneous expenses, is assumed to be 10% of the annual initial capital cost [43]. The annual operation and maintenance cost, which mainly includes the repair cost of the system, is planned to repeat annually and is assumed to be 2% of the annual initial capital cost [43, 44].

3.2. Constraints. To ensure system reliability, the loss of power supply (δ_{LPS}) and excess energy (δ_{EX}) are used as the reliability indexes of the hybrid PWB generation system. δ_{LPS} is defined as the energy deficit in relation to the total power requirements of the water pump. During the period considered, it is defined using the following equation [45, 46]:

$$\delta_{\mathrm{LPS}} = \sum_{t=1}^{T}\left\{P_{\mathrm{pump}}(t) - \left[P_{\mathrm{w}}(t) + P_{\mathrm{pv}}(t) + P_{\mathrm{discharge}}(t)\eta_{\mathrm{out}}\right]\right\}, \tag{19}$$

where $P_{\mathrm{discharge}}(t)$ is the actual discharge power of the battery at time t (W).

Correspondingly, the δ_{EX} is defined as the excess energy, which is determined by using the following equation [47]:

$$\delta_{\mathrm{EX}} = \sum_{t=1}^{T}\left\{P_{\mathrm{w}}(t) + P_{\mathrm{pv}}(t) - \left[\frac{P_{\mathrm{charge}}(t)}{\eta_{\mathrm{in}}} + P_{\mathrm{pump}}(t)\right]\right\}, \tag{20}$$

where $P_{\mathrm{charge}}(t)$ is the actual charging power of the battery at time t (W).

In addition, the battery S_{oc} must meet the following constraints to avoid overcharging or overdischarging, which adversely affects the lifetime of the battery [23, 46]:

$$S_{\mathrm{OC}_{\min}} \le S_{\mathrm{OC}}(t) \le S_{\mathrm{OC}_{\max}}, \tag{21}$$

where $S_{\mathrm{OC}_{\max}}$ is the maximum allowable S_{oc} of the battery (%), while $S_{\mathrm{OC}_{\min}}$ is the minimum allowable S_{oc} of the battery (%).

During the charging or discharging process, when $S_{\mathrm{OC}}(t+\Delta t) < S_{\mathrm{OC}_{\min}}$ at time $t+\Delta t$, the actual discharge capacity of the batteries during Δt is expressed by using the following equation:

$$\Delta E_{\mathrm{discharge}} = N_{\mathrm{b}} E_{\mathrm{rate}}\left[S_{\mathrm{OC}}(t) - S_{\mathrm{OC}_{\min}}\right]\eta_{\mathrm{out}}. \tag{22}$$

When $S_{\mathrm{OC}}(t+\Delta t) > S_{\mathrm{OC}_{\max}}$ at time $t+\Delta t$, the actual charged capacity of the batteries during Δt is described by using the following equation:

$$\Delta E_{\mathrm{charge}} = N_{\mathrm{b}} E_{\mathrm{rate}}\frac{\left[S_{\mathrm{OC}_{\max}} - S_{\mathrm{OC}}(t)\right]}{\eta_{\mathrm{in}}}. \tag{23}$$

The improved PSO algorithm-based Son penalty function is used to obtain the optimal results. The numbers of PV panels and batteries and the rated power of the wind generator are used as the decision variables. The objective function is then minimized by searching the optimal combination of N_{pv}, N_{b}, and $P_{\mathrm{w,rate}}$.

The auxiliary function is expressed using the following equation:

$$F\left(N_{\mathrm{pv}}, N_{\mathrm{b}}, P_{\mathrm{w,rate}}, M_{\mathrm{p}}\right) = C_{\mathrm{T}} + M_{\mathrm{p}}\sum_{N=1}^{2}\left[\max\left(0, g_N\left(N_{\mathrm{pv}}, N_{\mathrm{b}}, P_{\mathrm{w,rate}}\right)\right)\right]^2, \tag{24}$$

where M_{p} is the penalty factor and N is the number of constraints; this then gives

$$\begin{aligned} g_1\left(N_{\mathrm{pv}}, N_{\mathrm{b}}, P_{\mathrm{w,rate}}\right) &= \sum_{t=1}^{T}\left\{P_{\mathrm{pump}}(t) - \left[P_{\mathrm{w}}(t) + P_{\mathrm{pv}}(t)\right.\right. \\ &\quad \left.\left. + P_{\mathrm{discharge}}(t)\eta_{\mathrm{out}}\right]\right\} - \delta_{\mathrm{LPS,max}} \le 0, \\ g_2\left(N_{\mathrm{pv}}, N_{\mathrm{b}}, P_{\mathrm{w,rate}}\right) &= \sum_{t=1}^{T}\left\{P_{\mathrm{w}}(t) + P_{\mathrm{pv}}(t)\right. \\ &\quad \left. - \left[\frac{P_{\mathrm{charge}}(t)}{\eta_{\mathrm{in}}} + P_{\mathrm{pump}}(t)\right]\right\} - \delta_{\mathrm{EX,max}} \le 0. \end{aligned} \tag{25}$$

3.3. Improved Particle Swarm Optimization Algorithm. The PSO algorithm is based on populations called swarms that are formed of particles, with each particle representing a potential approach to the problem. Particles move around in a multidimensional search space during flight. Each particle adjusts its position depending on its experience and that of adjoining particles. However, finding the optimal solution using the PSO requires significant effort due to the constantly moving particles and the need to evaluate the fitness at each new position [47]. To be more precise, the position of a particle i at moment k can be regarded as $xk\ i$ and the velocity as $vk\ i$. The position and velocity vectors are then stored during the processing of the algorithm at time k to update the population at time $k+1$. The PSO also utilizes the best position information, which is obtained from the particle, to update the current particle swarm at a particular time defined by $pk\ i$, and the best position is the particle location at a time defined by $pk\ g$. In the next iteration, the velocity and position of each particle are determined using the current velocity and position as expressed by equations (26) and (27):

$$v_{id}^{k+1} = \omega v_{id}^{k} + c_1 r_1\left(p_{id}^{k} - x_{id}^{k}\right) + c_2 r_2\left(p_{gd}^{k} - x_{id}^{k}\right), \tag{26}$$

$$x_{id}^{k+1} = x_{id}^{k} + v_{id}^{k+1}, \tag{27}$$

where ω is the inertia weight parameter, c_1 is the cognitive coefficient, c_2 is the social coefficient, and r_1 and r_2 are both random numbers between 0 and 1 [47, 48].

As the inertia weight particle inherits the previous flight velocity, the adjustment of the inertia weight value can be found between the global and local searching balance. The inertia weight parameter is improved by the linear weighting method [49]. The inertia weight parameter is defined in the following equation [37, 50]:

$$\omega = \omega_{\max} - k\frac{\omega_{\max} - \omega_{\min}}{K}, \tag{28}$$

where $\omega_{\max}$ is the maximum inertia weight and $\omega_{\min}$ is the minimum inertia weight.

Normally, the parameter ω ranges from 0.4 to 0.9 [49], k is the number of current iterations, and K is the maximum number of iterations.

3.4. Simulation Process. The simulations are developed in MATLAB R2014a. The flowchart of the optimization model is shown in Figure 3. The strategy block diagram is used to determine which hybrid system to run. When the wind power is equal to zero, the PV/battery system operates. When the PV power is equal to zero, the wind/battery system operates. If both the wind power and PV power are not equal to zero, the PV/wind/battery system comes into operation. The specific calculation process is as follows.

First, the parameters such as solar radiation, ambient temperature, wind speed, and other parameters are fed into the optimization model. Then, determine whether $P_{pv} + P_w \geq P_{pump}$. If $P_{pv} + P_w \geq P_{pump}$, the excess power is charged to the battery and the capacity of the battery is calculated using equation (12). Alternatively, the battery will discharge to balance the requirements of the load, and the discharge capacity is calculated using equation (11). Next, the battery $S_{OC}(t)$ is calculated using equations (9) and (10). If $S_{OCmin} \leq S_{OC}(t) \leq S_{OCmax}$, it follows that the battery is charging or discharging normally. If $S_{OC}(t) < S_{OCmin}$, there is an energy deficit in the system. If $S_{OC}(t) > S_{OCmax}$, there is an energy surplus. Next, the load loss and energy surplus are calculated for the period T. Finally, δ_{LPS} and δ_{EX} are obtained from equations (19) and (20). Second, the auxiliary function is evaluated and the optimal results are obtained.

4. Results and Discussion

The model applications are performed in Weinan, Shaanxi, China (34°95′N, 109°58′E). Tomatoes are irrigated in a greenhouse, and the growing period is from August to December. The water consumption intensity of the tomato is 4.4, 2.7, 1.2, 0.92, and 1.0 mm d^{-1} for each month in the growing period. The maximum water requirement occurs in August. Thus, the system components are optimized for the month of August. In addition, based on the local irrigation schedule and irrigation demand of tomatoes, the water pump has to operate for 10 h/day. The detailed technical specifications of the components are provided in Table 1.

The hourly solar radiation on the horizontal surface (Figure 4(a)) and the ambient temperature (Figure 4(b)) are measured using an AV6592 PV cell tester, as shown in Figure 4. The hourly wind speed is obtained from a meteorological station. The data are recorded every ten minutes, and the mean hourly value is used in this study, as shown in Figure 5. The input parameters for the optimization model are shown in Table 2, and Table 3 shows the parameters of the PSO algorithm. The cognitive coefficient and social coefficient are equal to 2.05 based on experience. Presimulations have showed that the fitness function value kept steady after about 37 iterations. The maximum of iterations is determined by the fitness function value. If the fitness function value does not change any longer during iteration, the iteration can be terminated. Therefore, the maximum of iterations is set as 200 to avoid wasting too much simulation time. A high particle velocity may prevent finding the optimal solution of the model and a low particle velocity will affect the convergence speed of the model; therefore, the particle velocity range is set as −3–3. Because the optimization problem in this study is relatively simple, the number of particles is set as 20 and the population is set as 1–70, respectively.

4.1. Optimization Results. The convergence curve of the PSO algorithm is shown in Figure 6. The annual cost does not present any variations from iteration 37 onwards.

The optimization simulation results are two PV panels and two batteries, and the rated power of the wind generator is 375 W. The annual cost of this configuration is 1281.6 RMB.

4.2. Field Experiment Results. Field experiment is conducted on 1–15 August, 2017, in the greenhouse growing tomatoes located at the Agricultural Science Research Institute, Weinan, Shaanxi, China. As shown in Figure 7, the hybrid PV-wind controller is used to measure the power generated by the PV panels and wind generator, as well as the hourly power required by the water pumping system.

The hourly performance of the hybrid system based on the optimized configuration is illustrated in Figure 8.

While the water pump is working, the S_{OC} decreases at first and then increases. The reason is that the PV and wind power generation capacity is not sufficient to meet the load power requirements at the beginning. At this time, the battery needs to provide electricity for part of the load power requirements, and thus the battery S_{OC} decreases gradually. However, after the S_{OC} reaches its minimum value, the battery S_{OC} begins to increase. This is because the PV and wind power generation capacity goes up gradually and is able to meet the load power requirements. With the increase in PV and wind power generation, their sum begins to exceed the load power requirements. In consequence, the battery S_{OC} rises gradually before reaching its maximum value. These results show that the battery switches between charging and discharging states continuously. It is evident that the optimal configuration of the PV panels, wind generator, and batteries can ensure 10 h working time per day for the device providing good conditions.

The total output power of the PV panels and wind generator during 15 d are 41.478 kW (Figure 8(a)) and 6.235 kW (Figure 8(b)), respectively. The total load power of the pump is 36.965 kW (Figure 8(c)). The optimal configuration of the PV panels, wind generator, and batteries ensures the drip irrigation system remains fully functional. The S_{OC} of the battery is often greater than 50% during the 15 d (Figure 8(d)).

4.3. Discussion. This work focuses on establishing an optimization model to minimize the annual cost of a PWB generation system while ensuring the reliability of the system. Also, the climatic conditions and crop irrigation

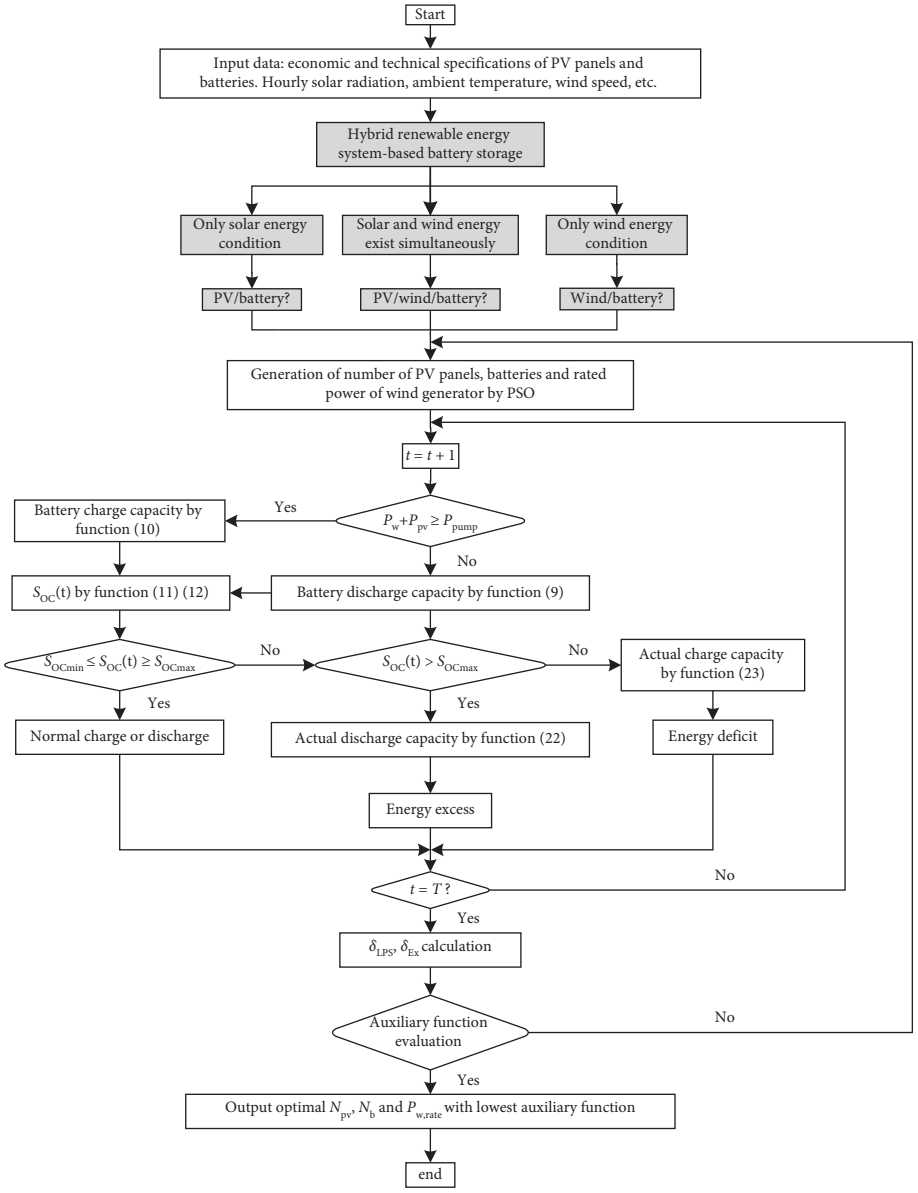

Figure 3: The flowchart of the optimization model for the hybrid PV-wind water pumping system.

Table 1: Component specifications.

Components	Type	Specification details
PV panels	CS5M32-260	Peak power: 260 W Peak voltage: 49.71 V Peak current: 5.25 A
Wind generator	NE-400	Rated voltage: 24 V Rated wind speed: 10 m/s
Battery	190H52 valve regulated lead battery	Rated capacity: 1440 Wh Rated voltage: 12 V
Controller	Hybrid solar wind controller	Voltage: 24–160 V Current: 0–20 A
Photovoltaic cell tester	AV6592	Voltage test precision: 0.01 V Current test precision: 0.001 A Test range of the maximum power: 0.1–500 W

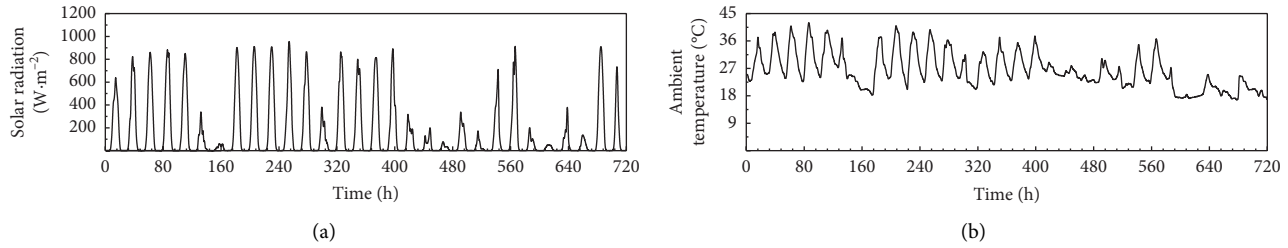

Figure 4: Optimization model input parameters for solar radiation (a) and ambient temperature (b) in August.

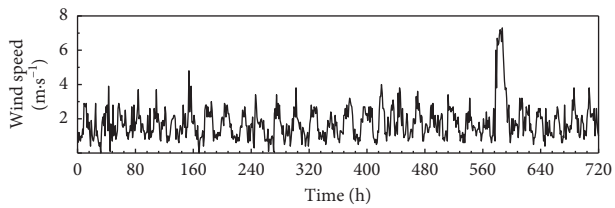

Figure 5: Optimization model input parameters for wind speed in August.

Table 2: Input parameters of the optimization model for simulation.

Input parameters	Value
Irrigation area (m^2)	350
Irrigation duration (h)	8
Irrigation water use efficiency (%)	80
Water pump efficiency (%)	40
Water pump head (m)	20
Water density (g m^{-3})	1
Acceleration of gravity (m s^{-2})	9.8
Cost of PV (RMB)	1000
PV panel area (m^2)	1.5
Solar radiation (W m^{-2})	Figure 4(a)
Ambient temperature (°C)	Figure 4(b)
Temperature coefficient	−0.34
Reference cell temperature (°C)	25
Cost of battery (RMB)	600
Cost of controller (RMB)	1600
Nominal operation cell temperature (°C)	45
PV panel efficiency at reference	16.6
Charge efficiency of battery (%)	90
Discharge efficiency of battery (%)	85
Initial state of charge (%)	60
Minimum S_{OC} value (%)	20
Maximum S_{OC} value (%)	80
Cost of wind generator (RMB W^{-1})	3.7
Cut-in value (m s^{-1})	1.5
Cut-out value (m s^{-1})	15
Rated wind speed (m s^{-1})	10
Wind speed (m s^{-1})	Figure 5
Real interest rate (%)	3.1
Project lifetime (year)	20
Inflation rate (%)	3.5
Desired δ_{LPS} value (W)	0
Desired δ_{EX} value (W)	0

Table 3: Parameters of the particle swarm optimization algorithm.

Parameters	Value
Cognitive coefficient	2.05
Social coefficient	2.05
Maximum number of iterations	200
Number of particles	20
Maximum particle velocity	3
Minimum particle velocity	−3
Upper population	70
Lower population	1

schedule are parameterized in the model. This study differs from that of Yahyaoui et al. [1, 2], who used the principle of energy supply and demand balance to determine the optimal components of system. In addition, in the present model, the annual cost is calculated using a dynamic approach, which consists of not only the initial capital cost but also the replacement cost, installation cost, and the costs of operation and maintenance. The constraints of the present model are the loss of power supply (δ_{LPS}) and excess energy (δ_{EX}). Compared with the work of Bakelli et al. [46], Olcan [23], and Aziz et al. [51], the present work also uses δ_{EX} to obtain more accurate optimization results. Furthermore, this study employs the penalty function to transform the constrained optimization problem into an unconstrained problem, which is consistent with a previous study that focused on a hybrid diesel-organic Rankine cycle (ORC)/PV system [47].

Moreover, the results of the field experiment demonstrate the applicability of the proposed model to a PWB generation system to determine the optimal components and achieve reliability. The optimization model is applied to a water pumping system in a greenhouse in Weinan for

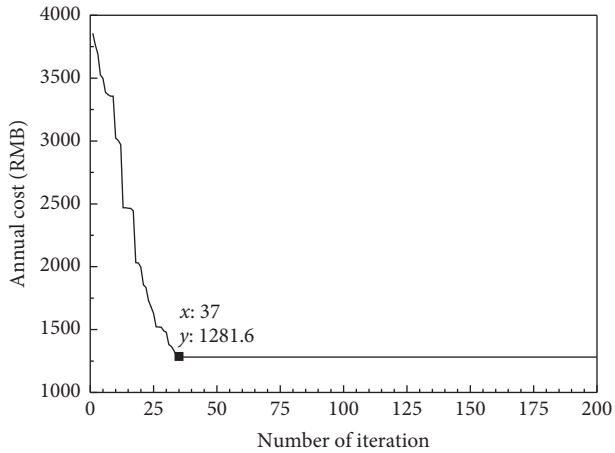

Figure 6: Optimization model convergence curve for the particle swarm optimization algorithm.

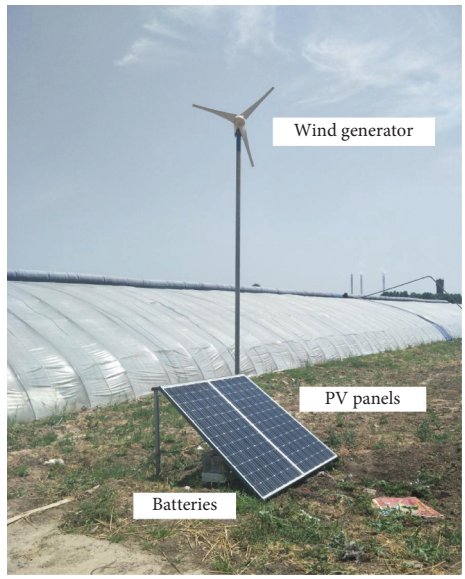

Figure 7: The hybrid PV-wind-battery water pumping system used for drip irrigation in a greenhouse.

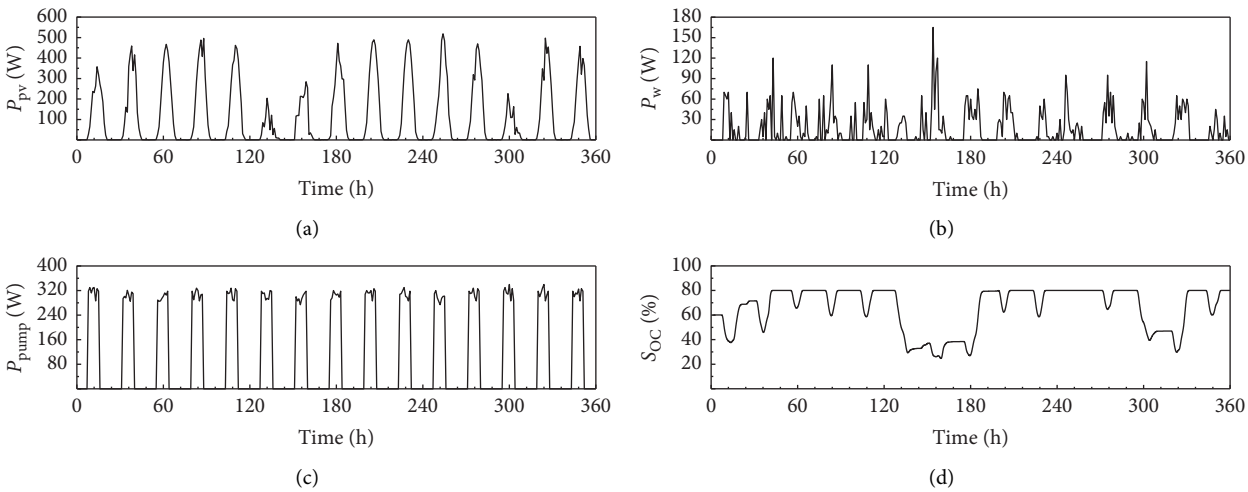

Figure 8: Hourly output power of PV panels (a) and wind generator (b), load power of the pump (c), and the battery S_{oc} (d) of the hybrid PV-wind-battery water pumping system based on the optimal configuration.

irrigating tomatoes. However, the model is equally applicable to other locations and other irrigated crops. Because the climatic conditions (e.g., solar radiation, ambient temperature, and wind speed) and irrigation schedule of crops (e.g., irrigation amount and irrigation duration) are parametric design in the model.

In addition, the loss of power supply affects the system components and annual costs. The optimal configuration of the PWB system depends on the water requirements and the type and moisture sensitivity of the crops during the critical period. Since the model considers the operating conditions such as the number of cloudy days, the model that reduces the loss of power supply can be used to ensure design redundancy to meet the agricultural production requirements.

5. Conclusions

A universal sizing optimization model for a hybrid PWB generation system was established, and the climatic conditions and crop irrigation schedule were parameterized in the model. Minimization of the annual cost was the objective function. The constraints include the battery S_{OC} and the power supply reliability, which is composed of the loss of power supply (δ_{LPS}) and excess energy (δ_{EX}). The numbers of PV panels and batteries, as well as the rated power of the wind generator, were the decision variables. Measured climatic data and the water requirement for irrigated tomatoes were used in the optimization model. The optimal configuration of the proposed hybrid PWB generation system was obtained. Finally, the performance of the system was tested in a greenhouse in Weinan for 15 d. The field results showed that the total output power of the PV panels and wind generator were 41.478 kW and 6.235 kW, respectively. The total load power of the pump was 36.965 kW. The results demonstrated that the optimized system was able to meet the power requirements of the water pumping system, thereby validating the size optimization model.

Data Availability

The data used to support the findings of this study are included within the article.

Conflicts of Interest

The authors declare no conflicts of interest.

Acknowledgments

This work was supported by the National Science and Technology Support Program (2015BAD22B01-02), "111" Program of the National International Office (B12007), and Innovation Program of Yangling Demonstration Zone (2017CXY-09).

References

[1] I. Yahyaoui, A. Atieh, A. Serna, and F. Tadeo, "Sensitivity analysis for photovoltaic water pumping systems: energetic and economic studies," *Energy Conversion and Management*, vol. 135, pp. 402–415, 2017.

[2] I. Yahyaoui, A. Atieh, F. Tadeo, and G. M. Tina, "Energetic and economic sensitivity analysis for photovoltaic water pumping systems," *Solar Energy*, vol. 144, pp. 376–391, 2017.

[3] C. Shang, D. Srinivasan, and T. Reindl, "An improved particle swarm optimisation algorithm applied to battery sizing for stand-alone hybrid power systems," *International Journal of Electrical Power & Energy Systems*, vol. 74, pp. 104–117, 2016.

[4] J. J. Halama, B. L. Barnhart, R. E. Kennedy et al., "Improved soil temperature modeling using spatially explicit solar energy drivers," *Water*, vol. 10, no. 10, pp. 3–15, 2018.

[5] G. Li, Y. Jin, M. W. Akram, and X. Chen, "Research and current status of the solar photovoltaic water pumping system—a review," *Renewable and Sustainable Energy Reviews*, vol. 79, pp. 440–458, 2017.

[6] P. E. Campana, H. Li, J. Zhang, R. Zhang, J. Liu, and J. Yan, "Economic optimization of photovoltaic water pumping systems for irrigation," *Energy Conversion and Management*, vol. 95, pp. 32–41, 2015.

[7] S. Ahmadi and S. Abdi, "Application of the hybrid Big Bang-Big Crunch algorithm for optimal sizing of a stand-alone hybrid PV/wind/battery system," *Solar Energy*, vol. 134, pp. 366–374, 2016.

[8] A. B. Guzmán, R. B. Vicencio, J. A. Ardila-Rey, E. N. Ahumada, A. G. Araya, and G. A. A. Moreno, "Cost-effective methodology for sizing solar PV systems for existing irrigation facilities in Chile," *Energies*, vol. 11, p. 1853, 2018.

[9] W. Lu, Y. Zhang, H. Fang, X. Ke, and Q. Yang, "Modelling and experimental verification of the thermal performance of an active solar heat storage-release system in a Chinese solar greenhouse," *Biosystems Engineering*, vol. 160, pp. 12–24, 2017.

[10] R. Wang, G. Li, M. Ming, G. Wu, and L. Wang, "An efficient multi-objective model and algorithm for sizing a stand-alone hybrid renewable energy system," *Energy*, vol. 141, pp. 2288–2299, 2017.

[11] D. Xu, S. Du, and L. G. van Willigenburg, "Optimal control of Chinese solar greenhouse cultivation," *Biosystems Engineering*, vol. 171, pp. 205–219, 2018.

[12] W. Zhou, C. Lou, Z. Li, L. Lu, and H. Yang, "Current status of research on optimum sizing of stand-alone hybrid solar-wind power generation systems," *Applied Energy*, vol. 87, no. 2, pp. 380–389, 2010.

[13] R. Kumar, R. A. Gupta, and A. K. Bansal, "Economic analysis and power management of a stand-alone wind/photovoltaic hybrid energy system using biogeography based optimization algorithm," *Swarm and Evolutionary Computation*, vol. 8, pp. 33–43, 2013.

[14] M. H. Amrillahi and S. M. T. Bathaee, "Techno-economic optimization of hybrid photovoltaic/wind generation together with energy storage system in a stand-alone micro-grid subjected to demand response," *Applied Energy*, vol. 202, pp. 66–77, 2017.

[15] Z. W. Geem, "Size optimization for a hybrid photovoltaic-wind energy system," *International Journal of Electrical Power & Energy Systems*, vol. 42, no. 1, pp. 448–451, 2012.

[16] E. D. Castronuovo and J. A. P. Lopes, "Optimal operation and hydro storage sizing of a wind-hydro power plant," *International Journal of Electrical Power & Energy Systems*, vol. 26, no. 10, pp. 771–778, 2004.

[17] S. S. Chandel, M. N. Naik, and R. Chandel, "Review of performance studies of direct coupled photovoltaic water pumping systems and case study," *Renewable and Sustainable Energy Reviews*, vol. 76, pp. 163–175, 2017.

[18] T. Khatib, A. Mohamed, and K. Sopian, "A review of photovoltaic systems size optimization techniques," *Renewable and Sustainable Energy Reviews*, vol. 22, pp. 454–465, 2013.

[19] D. H. Muhsen, T. Khatib, and H. T. Haider, "A feasibility and load sensitivity analysis of photovoltaic water pumping system with battery and diesel generator," *Energy Conversion and Management*, vol. 148, pp. 287–304, 2017.

[20] G. B. Shrestha and L. Goel, "A study on optimal sizing of stand-alone photovoltaic stations," *IEEE Transactions on Energy Conversion*, vol. 13, no. 4, pp. 373–378, 1998.

[21] C. Zhang, P. E. Campana, J. Yang, and J. Yan, "Economic performance of photovoltaic water pumping systems with business model innovation in China," *Energy Conversion and Management*, vol. 133, pp. 498–510, 2017.

[22] I. Tégani, A. Aboubou, M. Y. Ayad, M. Becherif, R. Saadi, and O. Kraa, "Optimal sizing design and energy management of stand-alone photovoltaic/wind generator systems," *Energy Procedia*, vol. 50, pp. 163–170, 2014.

[23] C. Olcan, "Multi-objective analytical model for optimal sizing of stand-alone photovoltaic water pumping systems," *Energy Conversion and Management*, vol. 100, pp. 358–369, 2015.

[24] R. Lamedica, E. Santini, A. Ruvio, L. Palagi, and I. Rossetta, "A MILP methodology to optimize sizing of PV—wind renewable energy systems," *Energy*, vol. 165, pp. 385–398, 2018.

[25] A. Maleki, "Design and optimization of autonomous solar-wind-reverse osmosis desalination systems coupling battery and hydrogen energy storage by an improved bee algorithm," *Desalination*, vol. 435, pp. 221–234, 2018.

[26] W. Zhang, A. Maleki, and M. A. Rosen, "A heuristic-based approach for optimizing a small independent solar and wind hybrid power scheme incorporating load forecasting," *Journal of Cleaner Production*, vol. 241, p. 117920, 2019.

[27] W. Zhang, A. Maleki, M. A. Rosen, and J. Liu, "Sizing a stand-alone solar-wind-hydrogen energy system using weather forecasting and a hybrid search optimization algorithm," *Energy Conversion and Management*, vol. 180, pp. 609–621, 2019.

[28] A. Maleki, "Optimal operation of a grid-connected fuel cell based combined heat and power systems using particle swarm optimisation for residential sector," *International Journal of Ambient Energy*, pp. 1–20, 2019.

[29] A. Maleki, "Modeling and optimum design of an off-grid PV/WT/FC/diesel hybrid system considering different fuel prices," *International Journal of Low-Carbon Technologies*, vol. 13, no. 2, pp. 140–147, 2018.

[30] A. Mellit, M. Benghanem, and S. A. Kalogirou, "Modeling and simulation of a stand-alone photovoltaic system using an adaptive artificial neural network: proposition for a new sizing procedure," *Renewable Energy*, vol. 32, no. 2, pp. 285–313, 2007.

[31] S. Sinha and S. S. Chandel, "Review of recent trends in optimization techniques for solar photovoltaic-wind based hybrid energy systems," *Renewable and Sustainable Energy Reviews*, vol. 50, pp. 755–769, 2015.

[32] A. Khare and S. Rangnekar, "A review of particle swarm optimization and its applications in solar photovoltaic system," *Applied Soft Computing*, vol. 13, no. 5, pp. 2997–3006, 2013.

[33] E. Riccietti, S. Bellavia, and S. Sello, "Sequential linear programming and particle swarm optimization for the optimization of energy districts," *Engineering Optimization*, vol. 51, no. 1, pp. 84–100, 2018.

[34] T. Cura, "A particle swarm optimization approach to clustering," *Expert Systems with Applications*, vol. 39, no. 1, pp. 1582–1588, 2012.

[35] M. Fadaee and M. A. M. Radzi, "Multi-objective optimization of a stand-alone hybrid renewable energy system by using evolutionary algorithms: a review," *Renewable and Sustainable Energy Reviews*, vol. 16, no. 5, pp. 3364–3369, 2012.

[36] J. Kennedy and R. Eberhart, "Particle swarm optimization," *IEEE Transactions on Evolutionary Computation*, vol. 4, pp. 1942–1948, 1995.

[37] M. Joana, R. P. V. Faria, I. B. R. Nogueira, J. M. Loureiro, and A. M. Ribeiro, "Optimization strategies for chiral separation by true moving bed chromatography using particles swarm optimization (PSO) and new parallel PSO variant," *Computers and Chemical Engineering*, vol. 123, pp. 344–356, 2019.

[38] J. Wang, H. Cai, H. Li, and X. Chen, "Study and evaluation of the calculation methods of reference crop evapotranspiration in solar-heated greenhouse," *Journal of Irrigation and Drainage Engineering-ASCE*, vol. 26, no. 6, pp. 11–14, 2006.

[39] A. Maleki and F. Pourfayaz, "Optimal sizing of autonomous hybrid photovoltaic/wind/battery power system with LPSP technology by using evolutionary algorithms," *Solar Energy*, vol. 115, pp. 471–483, 2015.

[40] R. Senol, "An analysis of solar energy and irrigation systems in Turkey," *Energy Policy*, vol. 47, pp. 478–486, 2012.

[41] D. H. Muhsen, T. Khatib, and T. E. Abdulabbas, "Sizing of a standalone photovoltaic water pumping system using hybrid multi-criteria decision making methods," *Solar Energy*, vol. 159, pp. 1003–1015, 2018.

[42] A. A. Ghoneim, "Design optimization of photovoltaic powered water pumping systems," *Energy Conversion and Management*, vol. 47, no. 11-12, pp. 1449–1463, 2006.

[43] H. Yang, W. Zhou, L. Lu, and Z. Fang, "Optimal sizing method for stand-alone hybrid solar-wind system with LPSP technology by using genetic algorithm," *Solar Energy*, vol. 82, no. 4, pp. 354–367, 2008.

[44] K. Bataineh and D. Dalalah, "Optimal configuration for design of stand-alone PV system," *Smart Grid and Renewable Energy*, vol. 3, no. 2, pp. 139–147, 2012.

[45] S. Ould-Amrouche, D. Rekioua, and A. Hamidat, "Modelling photovoltaic water pumping systems and evaluation of their CO_2 emissions mitigation potential," *Applied Energy*, vol. 87, no. 11, pp. 3451–3459, 2010.

[46] Y. Bakelli, A. Hadj Arab, and B. Azoui, "Optimal sizing of photovoltaic pumping system with water tank storage using LPSP concept," *Solar Energy*, vol. 85, no. 2, pp. 288–294, 2011.

[47] N. A. L. Galindo, L. S. M. Castellanos, E. E. S. Lora, and V. R. M. Cobas, "Optimum design of a hybrid diesel-ORC/photovoltaic system using PSO: case study for the city of Cujubim, Brazil," *Energy*, vol. 142, pp. 33–45, 2018.

[48] M. Mohammadi, S. H. Hosseinian, and G. B. Gharehpetian, "Optimization of hybrid solar energy sources/wind turbine systems integrated to utility grids as microgrid (MG) under pool/bilateral/hybrid electricity market using PSO," *Solar Energy*, vol. 86, no. 1, pp. 112–125, 2012.

[49] M. Sharafi and T. Y. ELMekkawy, "Multi-objective optimal design of hybrid renewable energy systems using PSO-simulation based approach," *Renewable Energy*, vol. 68, pp. 67–79, 2014.

[50] Z. Li, "Critical technology in solving multi-objective particle swarm optimization algorithm," *Journal of Communication and Computer*, vol. 11, pp. 100–103, 2014.

[51] N. I. A. Aziz, S. I. Sulaiman, S. Shaari, I. Musirin, and K. Sopian, "Optimal sizing of stand-alone photovoltaic system by minimizing the loss of power supply probability," *Solar Energy*, vol. 150, pp. 220–228, 2017.